# Thrust wedge tectonics and strike-slip faulting in the Sierra Nacimiento, New Mexico

Caleb J. Pollock[1]*, Kevin G. Stewart[1], James P. Hibbard[2],
Laura Wallace[1]**, and Ruben A. Giral[1]

[1]*Department of Geological Sciences, University of North Carolina, Chapel Hill, NC 27599*
[2]*Department of Marine, Earth and, Atmospheric Sciences, North Carolina State University, Raleigh, NC 27659*
**Current address: ExxonMobil Exploration Company, P.O. BOX 4778, Houston, TX 77210*
***Current address: Department of Geology, University of California, Santa Cruz, CA 95064*

**Abstract**

The Laramide Sierra Nacimiento uplift in north-central New Mexico forms a 70-km-long segment of the eastern edge of the Colorado Plateau. The suite of structures that separate the plateau from the Sierra Nacimiento include high-angle reverse faults, thrust faults, steep normal faults, strike-slip faults, and north-to-northwest-trending folds. We have developed a new structural model for the central part of the Sierra Nacimiento, based on detailed mapping and gravity modeling.

Dextral slip followed by uplift has endured as the preferred kinematic model of this uplift for several decades. New mapping, however, shows that an allochthonous wedge of crystalline basement has been thrust underneath the sedimentary section west of the uplift. Field data and gravity modeling indicate that the wedge was transported along a low-angle thrust fault and that high-angle faults exposed to the east most likely root into the gently dipping master thrust. The high-angle reverse faults and thrust faults are associated with an episode of subhorizontal tectonic shortening.

Estimates of the magnitude of strike-slip motion along the Nacimiento fault from previous workers range from approximately 2 to 30 km. The only fault in our area that appears to have had significant strike-slip motion is the high-angle fault separating the basement wedge from the main basement uplift to the east. The wedge contains Precambrian Joaquin granite, which is juxtaposed against Precambrian San Miguel gneiss east of the fault. The nearest exposure of Joaquin granite on the east side of this fault is 6 km south of the wedge, and the farthest is 18 km from the wedge, thus constraining the amount of dextral slip. Our interpretation of the structural data in this area indicates that the strike-slip motion occurred before the main episode of Laramide shortening and could be related to Proterozoic deformation, the late Paleozoic Ancestral Rocky Mountain orogeny, or an early phase of Laramide deformation.

## Introduction

The Sierra Nacimiento is a basement-involved Laramide uplift located in north-central New Mexico near the southern terminus of the Rocky Mountains. The interpretation of the structure of the Sierra Nacimiento has changed considerably since the earliest investigations. Renick (1931) first described the Sierra Nacimiento as an overthrust block bounded on the west by a complex system of both high-angle reverse and thrust faults. More recent studies by Baltz (1967), Woodward (1987), and Cather (1999) interpret the structure as the result of dextral transpression. A set of north-northwest plunging, broad, en echelon folds in the adjacent San Juan Basin were cited by Kelley (1955) and Baltz (1967) as evidence for early dextral wrench faulting. In their model subsequent west-vergent reverse faulting uplifted the crystalline basement, folded the sedimentary cover in the footwall of the Nacimiento fault system, and refolded the echelon folds (Woodward 1987). Similarly, Chapin and Cather (1983) cite the en echelon folds of the San Juan Basin as evidence for dextral displacement on the Nacimiento fault and faults to the east. Studies of zero-isopach contours of San Juan Basin Mesozoic strata show at least a possibility of dextral motion on the Nacimiento fault system (Woodward et al. 1997). The amount of offset, however, is controversial (Cather 1996; Woodward et al. 1997; Cather 1999) and has bearing on the hypothesis that north-northeast motion of the Colorado Plateau is responsible for Laramide shortening in the Wyoming province of the Rocky Mountains (Kelley 1955; Hamilton 1978; Karlstrom and Daniel 1993).

An earlier map of the west-central Sierra Nacimiento (Woodward et al. 1973a) shows two distinct bounding faults, the Nacimiento and the Pajarito faults, which terminate in proximity to one another. The lack of continuity between the Nacimiento and Pajarito faults restricts the amount of dip-slip or strike-slip displacement on these range-bounding faults. If there has been tens of kilometers of strike-slip motion along the western margin of the Sierra Nacimiento (e.g., Karlstrom and Daniel 1993) then these faults should be structurally linked.

Low-angle thrust faults in the sedimentary cover along the western margin of the uplift have been mapped by Woodward and coworkers (see Woodward 1987 for a summary), Stewart and Hibbard (1992), Giral (1995), as well as earlier workers. Stewart and Hibbard (1992) identified a low-angle thrust fault in the sedimentary cover that they interpreted as an early structure that preceded the main stages of uplift in the Sierra Nacimiento. Our more recent work has shown that this "thrust" is really a slump off the flank of a growing anticline that was transported to the east. This is contrary to the interpretation of this structure as a top-to-the-west thrust fault by Stewart and Hibbard (1992). Top-to-the-east faults were also mapped by Giral (1995). Woodward (1987) and Giral (1995) show that the Nacimiento fault crops out both as a high-angle west-directed reverse fault and a west-directed, low-angle thrust fault. Giral (1995) thought that west-directed low-angle faults of the Sierra Nacimiento were truncated by the later high-angle faults. However, the high-angle reverse and thrust faults may be either syngenetic and coeval (e.g., Woodward 1987) or the result of temporally distinct tectonic events. One possible event unrelated to Laramide deformation proposed by Giral (1995) is that Pliocene volcanism in the region reactivated the uplift. Slack and Campbell (1976) pro-

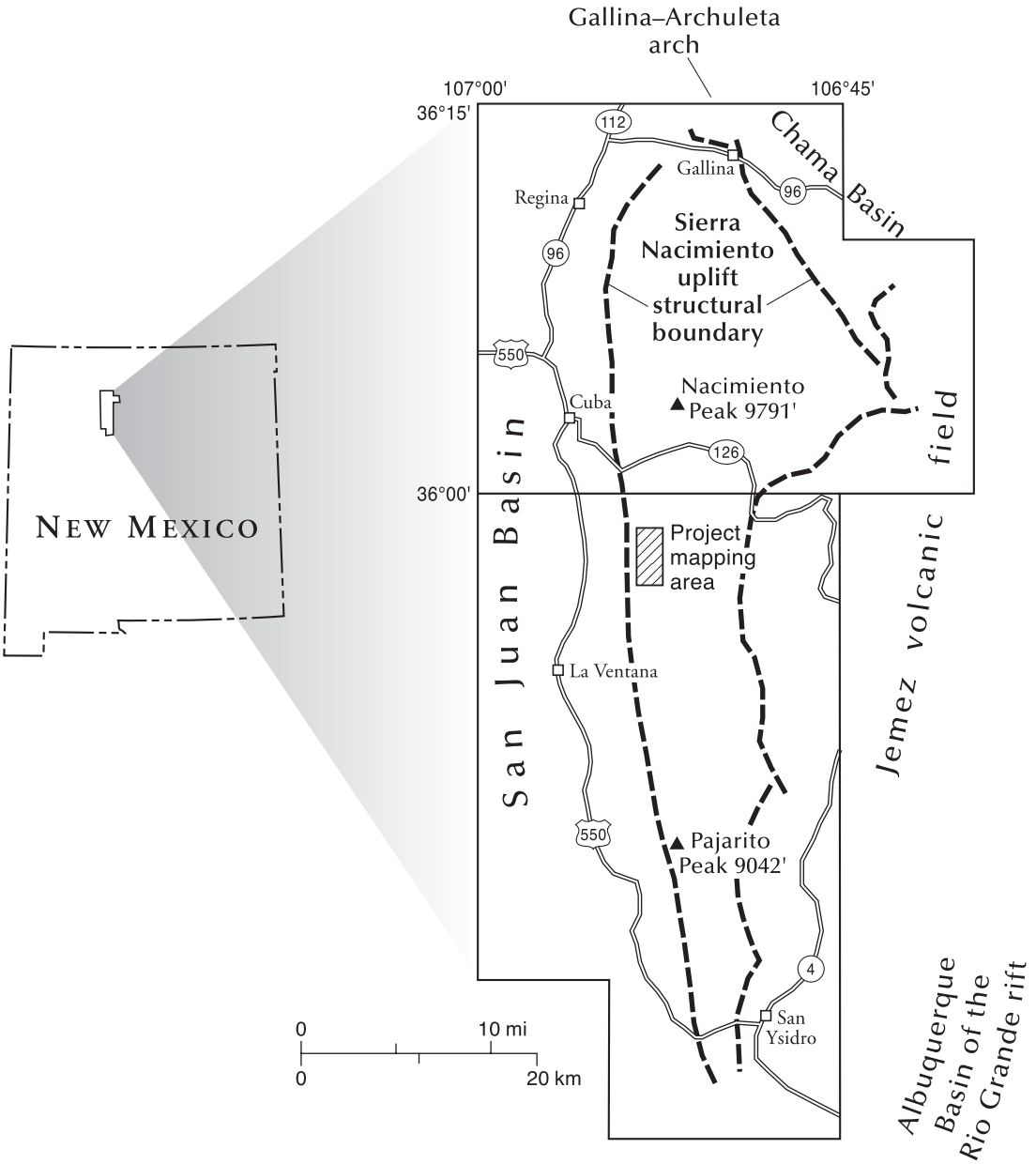


FIGURE 1—Map showing boundaries of the Sierra Nacimiento uplift and surrounding geologic features. Study area shown by shaded box. Modified from Woodward (1987).

posed the same event for motions in the Rio Puerco fault zone.

Several interpretations of the underlying structure of the Sierra Nacimiento have been published (Renick 1931; Baltz 1967; Woodward et al. 1972; Woodward 1987; Giral 1995; Yin and Ingersoll 1997); however, none of these earlier studies attempted to construct detailed and balanced cross sections. The purpose of this study is to determine the structural geology of the Nacimiento fault system using balanced cross sections based on new 1:6,000-scale geologic mapping of the central portion of the uplift and newly acquired gravity data. This study permits us to determine the structural relationship between the Nacimiento and Pajarito faults of Woodward (1987) and to constrain the amount of Laramide dip-slip motion across the Sierra Nacimiento uplift.

### General geology of the central part of the Sierra Nacimiento

The Sierra Nacimiento uplift is surrounded by an assemblage of geologically diverse features (Fig. 1). The San Juan Basin, which is part of the eastern margin of the Colorado Plateau, forms the western boundary of the uplift. The northern Sierra Nacimiento terminates in the Gallina–Archuleta Arch, which forms the structural divide between the San Juan Basin and the Chama Basin to the northeast. The eastern margin of the uplift is marked by the Miocene to Quaternary Jemez volcanic field. Northeast-trending faults of the late Tertiary Rio Grande rift truncate the uplift to the southeast. At its southern end the uplift terminates in south-trending, gently plunging folds.

As is typical for many Laramide basement uplifts most of the visible structures associated with the Sierra Nacimiento are in the sedimentary cover. The strata of the San Juan Basin generally have gentle dips (Baltz 1967; Woodward 1987). Although adjacent to the uplifted basement they are tightly folded, forming a monocline (Fig. 2). The faults along the western side of the uplift include high-angle reverse faults, high-angle normal faults, strike-slip faults, and west-

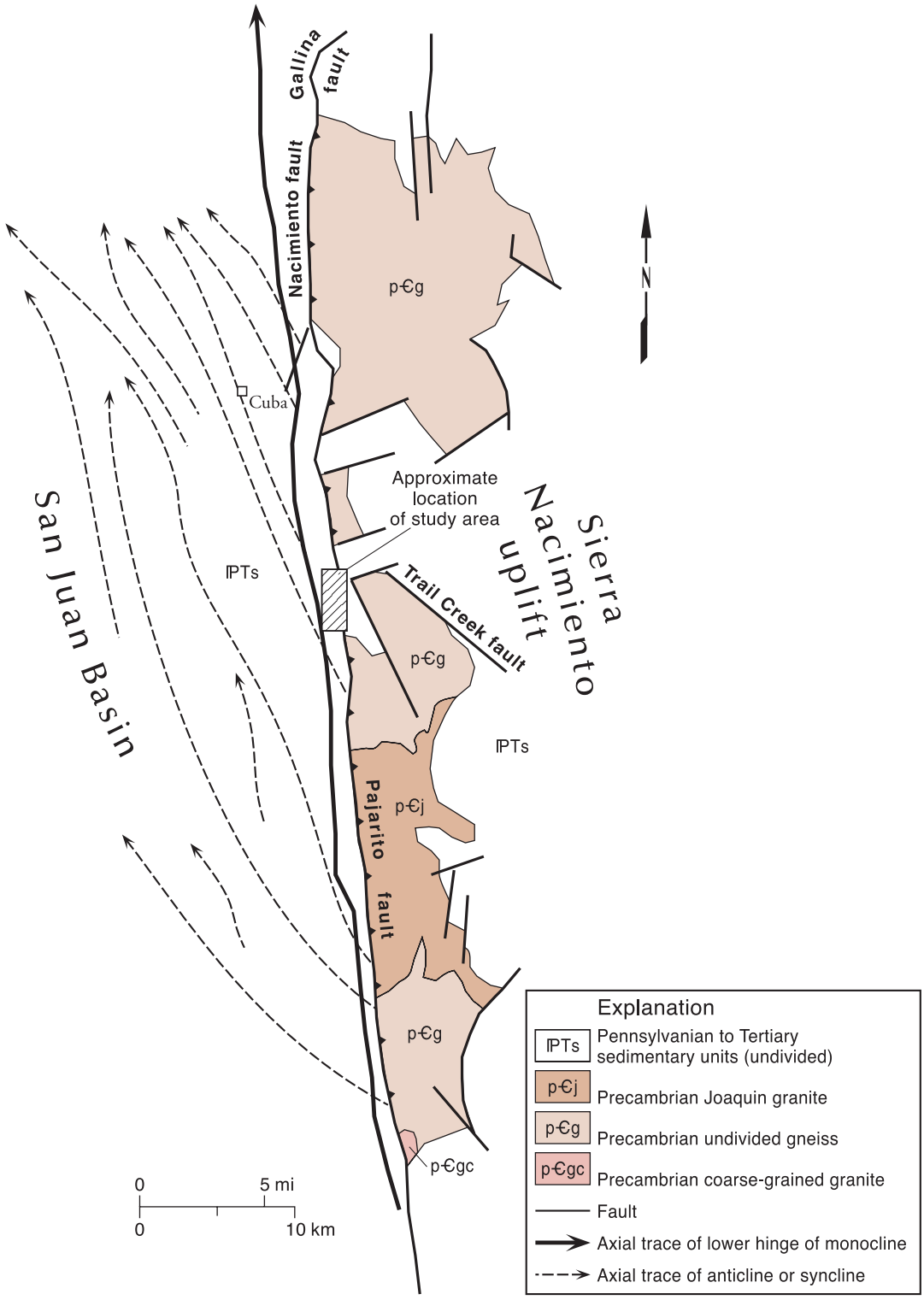


FIGURE 2—Generalized geologic map of Sierra Nacimiento uplift. Shown are major Precambrian basement units, undivided sedimentary units, major faults, and fold axial traces.

verging thrust faults (Renick 1931; Baltz 1967; Woodward et al. 1973a; Woodward 1987) including the Nacimiento and Pajarito faults of Woodward (1987), which are the primary range-bounding faults of the Sierra Nacimiento (Fig. 2). West of the uplift is a set of en echelon, gently north-northwest plunging folds (Kelley 1955; Baltz 1967). West-directed faults in the basement are seismically imaged in the eastern San Juan Basin (Taylor and Huffman 1998), as well as east-directed back-thrusts, which strike subparallel to the Nacimiento uplift (Giral 1995). Steeply dipping, east striking normal faults are also present in the central and southern parts of the uplift.

We mapped an area that includes parts of the San Pablo and La Ventana 7.5-min quadrangles (T19N R1W) secs. 1, 2, 11, 12, 13, 14, 22, 23, and 24 at a scale of 1: 6,000. This provided adequate resolution for the construction of detailed, bal-

anced cross sections. The map units in this field area range in age from Precambrian rocks to Holocene sediments. In the uplifted blocks of the Sierra Nacimiento, Precambrian igneous and metamorphic rocks are unconformably overlain by Pennsylvanian limestone and arkosic sandstone and by Permian shale, sandstone, and conglomerate. Mesozoic and Cenozoic sandstone, shale, evaporite, and limestone crop out in a steeply dipping belt in the footwall of the Nacimiento fault system and in flat-lying and gently folded outcrops adjacent to the mountain front (Baltz 1967). For a detailed description of the lithologic units of the eastern San Juan Basin and the Sierra Nacimiento uplift see Woodward (1987, pp. 9–48).

## Structural geology

### Continuity of the Nacimiento and Pajarito faults

Woodward et al. (1973a) show an approximately 1.5 km gap between the terminations of the Nacimiento and Pajarito faults near San Miguel Canyon. This interpretation limits the amount of displacement along the fault, particularly strike-slip displacement. Our interpretation, however, suggests that these faults are continuous, although there must be an abrupt change in dip of the fault.

Near San Miguel Springs the Abo Formation is faulted against the Triassic Salitral Shale Member of the Chinle Formation on a high-angle fault (Location 1 Sheet 1). This locality corresponds to the southern terminus of the Nacimiento fault as mapped by Woodward et al. (1973a). To the south an erosional window through a pediment deposit (Location 2 Sheet 1) shows that the Agua Zarca Member of the Chinle Formation can be extended beneath the pediment deposit to a north-south trending gully on the east side of the pediment deposit. On the east side of this gully the Permian Abo Formation is exposed. We interpret this truncation of the Agua Zarca to be a high-angle reverse fault, which is the southern continuation of the Nacimiento fault. The contact between the Permian Yeso Formation and Abo Formation in the footwall of the Nacimiento fault can be reasonably extrapolated to the same structural cutoff near Location 2 Sheet 1.

By extrapolating the basement-Abo contact beneath Location 3 Sheet 1 it can be shown that this outcrop is about 25 m above the basement-Abo contact. We think that the basement-Abo fault contact corresponds to the depositional basal contact of the Abo based on the stratigraphic thickness from the contact to the top of the Abo. West of this location there is an abrupt change in the orientation of the Abo Formation from N5°E 65°W to N10°E 30°E. Farther west the upper contact of the Abo Formation can be observed in a topographic saddle to the west of Location 3 Sheet 1. A measured section of the Abo Formation north of San Miguel Canyon shows that its undeformed thickness in the field area is 150 m. The juxtaposition of the upper and lower contacts of the Abo Formation and the abrupt change of orientation in the saddle indicate the presence of a fault. The sharp fold in the Abo is likely the result of draping of the sedimentary rocks during the faulting of underlying basement blocks but before the fault propagated into the sedimentary cover. We extrapolate the Nacimiento fault to Location 3 Sheet 1 and southward based on the above observations. Hereafter the structure bounding the Sierra Nacimiento uplift in this area will be referred to as the Nacimiento fault.

South of San Miguel Canyon the Nacimiento fault dips steeply to the east (~ 85°). To the north, the fault flattens to less than 30° and is locally horizontal (west of Location 4 Sheet 1). Woodward et al. (1973a) interpreted this flattening as evidence for an "upthrust" fault (e.g., Sanford 1959). This fault geometry requires that the hanging wall undergo extension and the small normal faults in the hanging wall of the Nacimiento fault (Location 4 Sheet 1) shown by Woodward et al. (1973a) were interpreted as having formed in this way (Fig. 3). Although we found evidence of landsliding in this area we were unable to recognize the normal faults reported by Woodward et al. (1973a). We will show later that the change in dip of the Nacimiento fault is probably associated with a ramp in the fault surface and does not require extension of the hanging wall.

### West-dipping backthrust

One of the prominent faults in the footwall strata is a west-dipping backthrust within the Permian Yeso Formation and Triassic Agua Zarca Member. Woodward et al. (1973a) originally mapped a more complex structure than is shown in our map (Location 5 Sheet 1). Throughout the map area the Agua Zarca Member contains channels of maroon, cross-bedded siltstone, and gray-green to maroon silty shale as well as minor maroon conglomerate. The fine-grained maroon beds present here were mapped as the Salitral Shale Member by Woodward et al. (1973a), but we interpret them as siltstones in the Agua Zarca Member. In our interpretation a simpler east-directed fault repeats part of the Permian Yeso and places the Yeso Formation over the Triassic Agua Zarca Member. This structure is either an early east-directed backthrust subsequently folded into its present position or an out-of-the-syncline thrust that formed during tightening of the footwall syncline. The timing for the development of this structure is unclear due to a lack of crosscutting relationships. Our preferred subsurface interpretation is a backthrust rooting in a structurally lower fault.

### Footwall culmination south of San Miguel Canyon

South of San Miguel Canyon is a pronounced culmination developed in the footwall strata (Sheet 1). The maximum structural relief is present in the center of the map area and extends northward to San Miguel Canyon and southward to the southern limit of the map area. At the center of this structure is a fault-bounded block of crystalline basement (Location 6 Sheet 1). This rock is a medium-grained, porphyritic pink granite with potassium feldspar phenocrysts as large as 1.5 cm. Biotite is present and commonly altered to chlorite near the fault zone. A weak foliation defined by alignment of the feldspar phenocrysts is locally present and is likely the result of magmatic flow during emplacement of the pluton. Woodward et al. (1973a) mapped this block as Precambrian San Miguel gneiss; however, the mineralogical composition of the granite (Table 1) at Location 6 on Sheet 1 matches well with the Joaquin granite as described in hand sample and thin section by Woodward (1987). The granite does not match the San Miguel gneiss texturally or mineralogically. The presence of chlorite and absence of biotite in the granite from Location 6 is attributable to low-grade alteration associated with faulting. A second candidate to match the fault-bounded block is the coarse-grained granite of Woodward (1987). Although the coarse-grained granite is compositionally similar to the fault-bounded block they are texturally distinct enough that we choose not to correlate them across the fault.

The western edge of the block is in contact with the Permian Abo Formation. At Location 6 Sheet 1 this contact is exposed and is oriented 176°, 68° W. Surrounding the contact both the Abo Formation and the Joaquin granite are intensely fractured, and many surfaces exhibit slickenlines. The contact itself is a cataclastic zone about 10 cm wide. We interpret this contact as a top-to-the-east bedding-parallel fault, which we call the Los Piños fault. The eastern edge of the block is in contact with both the Precambrian San

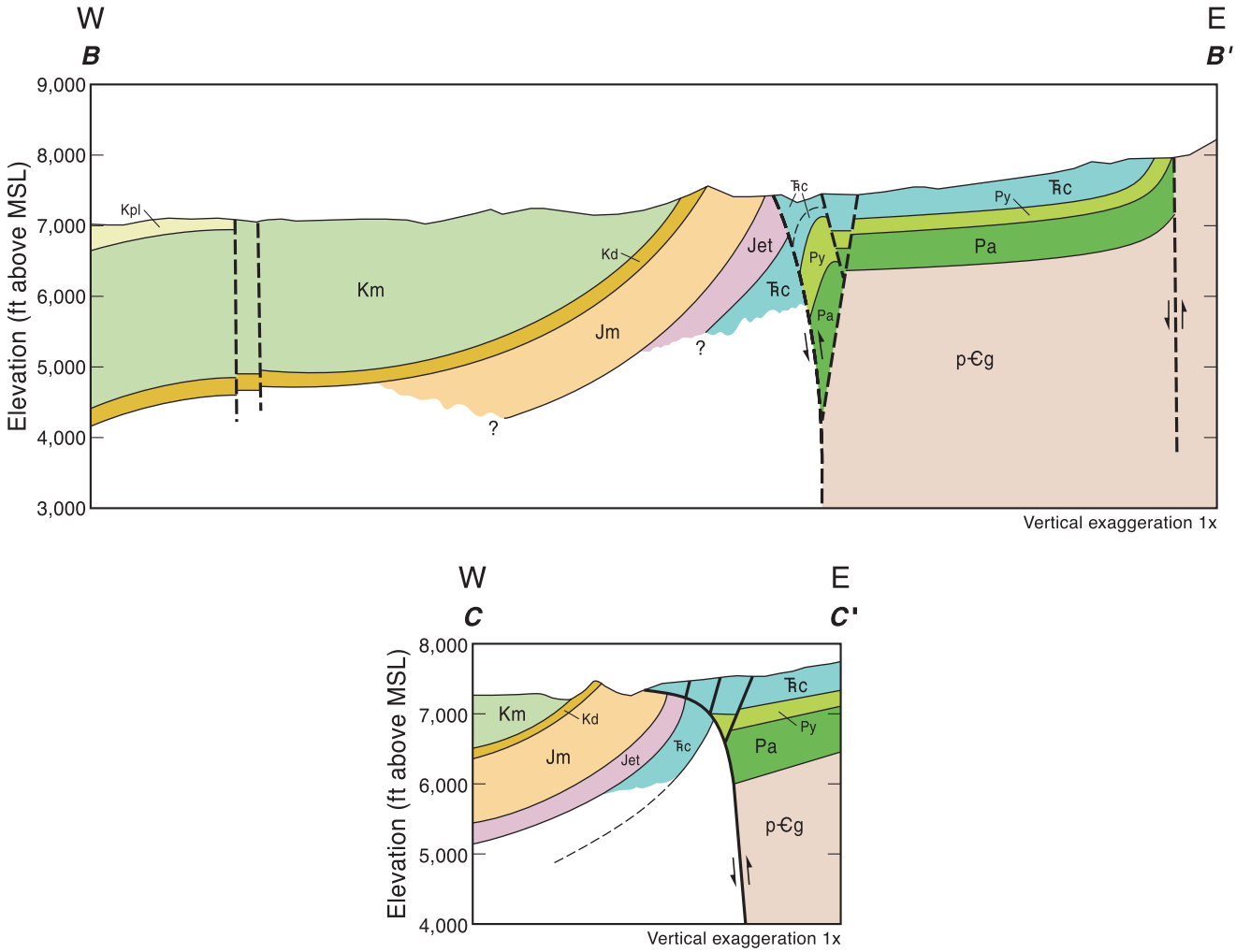


FIGURE 3—Cross sections **B–B′** and **C–C′** modified from Woodward et al. (1973a) of a part of the Sierra Nacimiento uplift based on the upthrust model of Sanford (1959). This model requires west-dipping normal faults in the hanging wall of the major thrust.

Miguel gneiss and the Pennsylvanian Madera Formation. The contact between the Joaquin granite and the San Miguel gneiss is not well exposed; however, material surrounding the contact is intensely fractured and is mapped by Woodward et al. (1973a) as a fault. We also believe this is a fault contact and represents the southward continuation of the Nacimiento fault. It is not clear if the outcrop of Madera is entirely fault bounded or if one of the contacts is a nonconformity. We interpret the contact between the Madera Formation and the Joaquin granite to be a nonconformity based on the lack of intense brecciation of the rocks near the contact. The contact between the Madera Formation and the San Miguel gneiss is interpreted as the southward extension of the Nacimiento fault based on the presence of brecciated limestone, slickensides, and epidote- and calcite-filled fractures.

Near the center of the culmination, Woodward and Schumacher (1973) mapped several small, east striking, dip-slip faults, which offset the contact between the Agua Zarca Member and Yeso Formation (Location 7 Sheet 1). A 0.75–1-m-thick, fine-grained, laminated limestone bed crops out continuously near the top of the Yeso Formation south of San Miguel Canyon. Because this bed shows no offset in the region of Woodward and Schumacher's faults, these structures were eliminated in Sheet 1.

### Kinematics of the mapped faults

Where the Nacimiento and Los Piños fault zones are exposed, they are typically 1–3 m wide (Fig. 4; Nacimiento, Locations 8 and 9; Los Piños, Location 6 Sheet 1) and show evidence of intense cataclasis. Both fault zones contain significant chlorite alteration and the Nacimiento fault zone locally contains massive quartz mineralization. We also observed the Nacimiento fault zone in several roadcuts to the south of our field area, which were mapped by Woodward and Schumacher (1973) in the La Ventana

TABLE 1—Composition of Joaquin granite and San Miguel gneiss (Woodward 1987) and granite outcrop from the footwall culmination of this study.

| | Joaquin granite (Woodward 1987) | granite outcrop (this study) | San Miguel gneiss (Woodward 1987) |
|---|---|---|---|
| microcline-microperthite | 40–50% | 40% | 11–32% |
| plagioclase | 18–21% | 14% | 29–36% |
| quartz | 24–37% | 34% | 25–30% |
| biotite + chlorite | 2–3% | 7% | 2–15% |
| muscovite | 1% | 3% | minor |
| other* | minor | 1% | minor |

* includes opaque minerals, sericite, zircon, sphene, and apatite

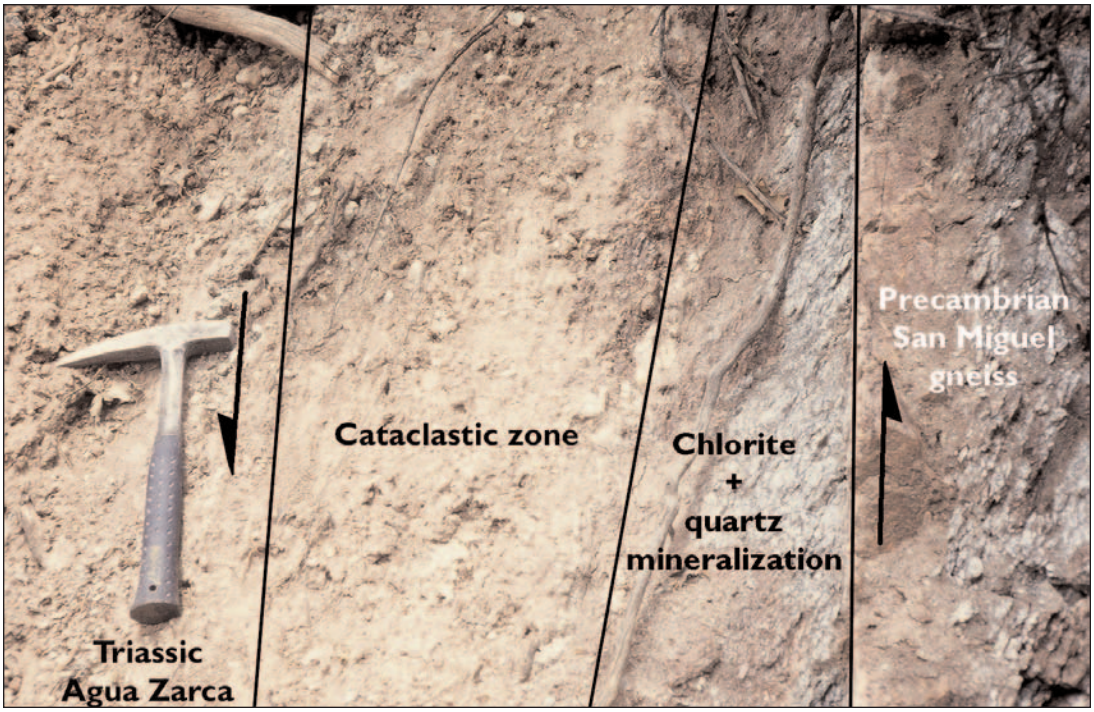


FIGURE 4—Photo of the Nacimiento fault from Location 8 Sheet 1 (view to the north). On the left is brittlely deformed Agua Zarca Member of the Chinle Formation. On the right is brecciated San Miguel gneiss.

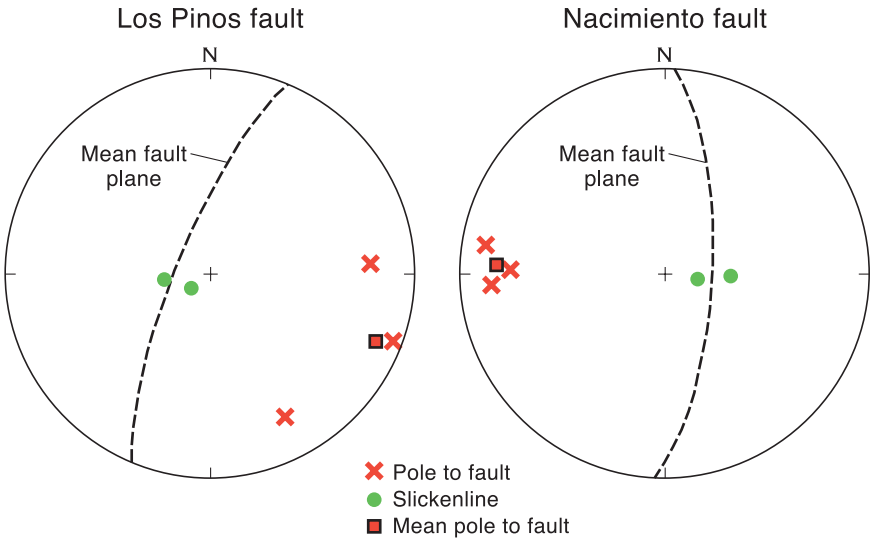


FIGURE 5—Equal-area plots of slickenline data from the Nacimiento and Los Piños faults. See Figure 8 for Los Piños fault.

7.5-min quadrangle (NE ¼ sec. 1 T18N R1W) and in the northeastern corner of the Ojo del Espiritu Santo (Holy Ghost Springs) portion of the Jemez land grant. In these locations the fault zone exhibited the same characteristics as we observed in our field area. Slip surfaces of the Nacimiento and Los Piños faults are poorly exposed in the field area, and kinematic indicators are rare. The four slickenlines measured display primarily dip slip (Fig. 5).

### Structural sections of the central Sierra Nacimiento

Cross sections of the Sierra Nacimiento using the upthrust model (Woodward et al. 1973a; Woodward and Schumacher 1973) are not balanced. Additionally, the upthrust model requires primarily vertical motion rather than the well-documented subhorizontal shortening common to most Laramide uplifts (Brown 1988). The cross sections presented for this study (Sheets 2, 3) show structures resulting from subhorizontal contraction and are balanced.

The cross sections shown on Sheets 2 and 3 are perpendicular to the trend of the Nacimiento fault. There is some structural thinning of the more ductile sedimentary units (e.g., Todilto Formation, the shale members of the Chinle Formation) near the mountain front, but this thinning is relatively minor. Although some sedimentary units may have been structurally thinned, it is difficult to document the amount of thinning; therefore, we have assumed constant thickness of the sedimentary units during folding. Based on this observation we assume that the dominant deformation mechanism in these rocks was flexural-slip folding and used the kink-band method (Suppe 1985) for construction of cross sections in sedimentary strata. The cross sections were drawn beyond our map boundary in order to develop a better model for the uplift. Surface geology for the extended portion of the sections is from Woodward and Schumacher (1973), Woodward et al. (1973a,b), and Woodward et al. (1974). Formation thicknesses were determined from outcrop, measured section, and well logs where available. The top of the basement in the hanging wall was located using outcrop (Woodward et al. 1974) and well data (Laughlin et al. 1983). Only basement rocks are balanced in these sections because much of the uplifted basement is stripped of sedimentary strata (Fig. 2). In all of the sections the basement rocks are assumed to have behaved as rigid, isotropic blocks that deformed primarily by brittle faulting. Bends in the fault surfaces are accommodated by brittle faulting and

rotation of the basement blocks not by folding of the basement (Erslev 1986); however, pervasive brittle failure of basement rocks can produce changes in the overall shape of a basement block (Evans 1986) as Erslev (1993) acknowledged. Both kinds of behavior are exhibited in our cross sections. Small faults and cataclastic deformation at the perimeter of basement blocks illustrated in Figure 6 are shown schematically in the cross sections with a crosshatch pattern.

In all of the cross sections the cover-basement interface in the foreland is treated as a décollement surface with top-to-the-east sense of motion. This structure is a "passive-roof" duplex (Banks and Warburton 1986), because the cover rocks have not been transported eastward, instead the basement rocks have been thrust westward underneath the sedimentary cover. This type of structure is also known as a "triangle zone" (Gordy et al. 1977). The passive roof thrust of this structure crops out as the Los Piños fault. Both sections A–A′ and B–B′ show the sedimentary strata of the footwall restored using bedding line-lengths. In the restored section the location of the Paleozoic sedimentary rocks in the hanging wall is arbitrary because of the missing strata in the center of the section. Additionally, it is not clear where displacement on the Los Piños fault ends so its eastern termination is queried in the cross sections.

**Cross sections**

Section A–A′ (Sheet 2) crosses the Nacimiento fault where it crops out as a low-angle fault. Section B–B′ (Sheet 3) crosses the high-angle Nacimiento fault at the north end of the footwall culmination. See Sheet 1 for the locations of the lines of section. The orientation of high-angle faults in cross sections A–A′ and B–B′ are from field data. Low-angle basement faults in our sections are similar to those seen in other Laramide uplifts (e.g., Wind River uplift, Wyoming; Smithson et al. 1979). Basement faults in our cross sections originate from a gently dipping (dip < 30°) master fault. Basement blocks are constructed so that, upon restoration, the blocks undergo a minimum change in shape and area.

**Cross section A–A′**—The structurally deepest fault of this section is the "master fault," which separates brittlely deformed allochthonous basement from undeformed basement (Sheet 2). The inferred dip of the master fault is approximately 30° to the east and becomes subhorizontal at the basement-cover interface. The basement wedge beneath the Los Piños fault probably contains many faults because this basement block has experienced the most shape change from the undeformed to deformed positions and thus the most internal strain. The inferred pervasive brittle failure in this block is indicated schematically in the section in yellow (Fig. 6).

In the center of the section is the block of Joaquin granite bounded by three faults. The "wedge-boundary fault" and the Nacimiento fault have top-to-the-west displacement; the Los Piños fault has top-to-the-east motion. The presence of the wedge-boundary fault is inferred from the sharp increase in the dip (> 10°) of the cover rocks. The Nacimiento fault reactivates part of an earlier dextral strike-slip fault that translated the block of Joaquin granite northward before the main phase of Laramide thrusting. The kinematics of this early phase of strike-slip faulting are discussed later. The Nacimiento fault displays a ramp-flat geometry; the fault steepens as it rises through the "strong" crystalline rocks and flattens into the "weak" sedimentary rocks (Sanford 1959; Prucha et al. 1965). The high cutoff angle of bedding in the footwall of the Nacimiento fault (Section $a_2$ Sheet 2) is due to folding of the sedimentary strata before faulting. This ramp-flat geometry of the fault is observable in the field and was the basis for Woodward et al.'s (1972) interpretation of the Nacimiento fault as an "upthrust." We believe that the Nacimiento fault flattens at depth yielding a flat-ramp-flat geometry.

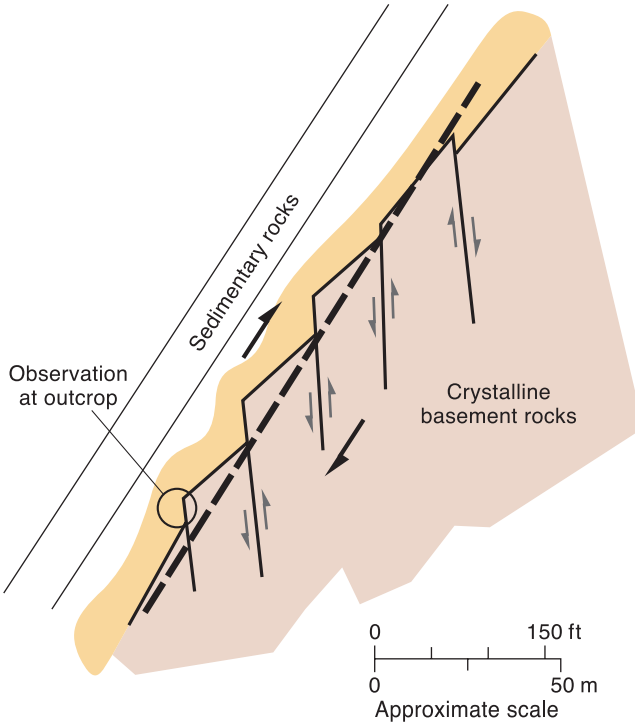


FIGURE 6—Schematic diagram of the Los Piños fault. Bold dashed line represents the average orientation of the fault zone. Cataclastic deformation of the sedimentary rocks in the fault zone is represented by the yellow. Gray arrows indicate motion on antithetic faults within brittlely deformed basement. One of these antithetic faults is observable at Location 6 Sheet 1.

Section A–A′ shows a fault we call the San Miguel fault that was previously mapped by Woodward et al. (1973a,b, 1974) as part of the Trail Creek fault. In these maps and sections the Trail Creek fault bounds a basement block on both the east and west, requiring a 180° bend in the fault around the north end of the block. We have chosen to separate the western trace of the Trail Creek fault into a separate fault called the San Miguel fault. Woodward et al. (1973a,b, 1974) showed the Trail Creek fault to have normal sense of motion. The fault dips nearly 90°, but we interpret it as a reverse fault because dip changes across the fault suggest concave-upward geometry.

**Cross section B–B′**—The faults present in section A–A′ are also present in section B–B′ (Sheet 3); however, the geometries of the faults and the blocks that they bound are different. For example, the footwall culmination shown on section B–B′ is a result of wedging of a thicker slice of Joaquin granite under the sedimentary cover than is inferred in section A–A′. The Los Piños fault, shown on both sections, is exposed at the surface in section B–B′ and is inferred to exist in the subsurface in section A–A′. The inferred cutoff of the Los Piños fault by the Nacimiento fault in section B–B′ is at a much higher elevation than in section A–A′, demonstrating the northerly plunge of the intersection of these faults of the Joaquin granite block. The "boundary fault," which defines the bottom of the wedge dips to the north as can be seen from comparing sections A–A′ and B–B′ and from the map (Sheet 1).

Two top-to-the-east faults are present in section B–B′. In addition to the Los Piños fault, an east-directed thrust fault cuts the Yeso Formation and Agua Zarca Member and is interpreted to be a splay off the Los Piños fault. Banks and

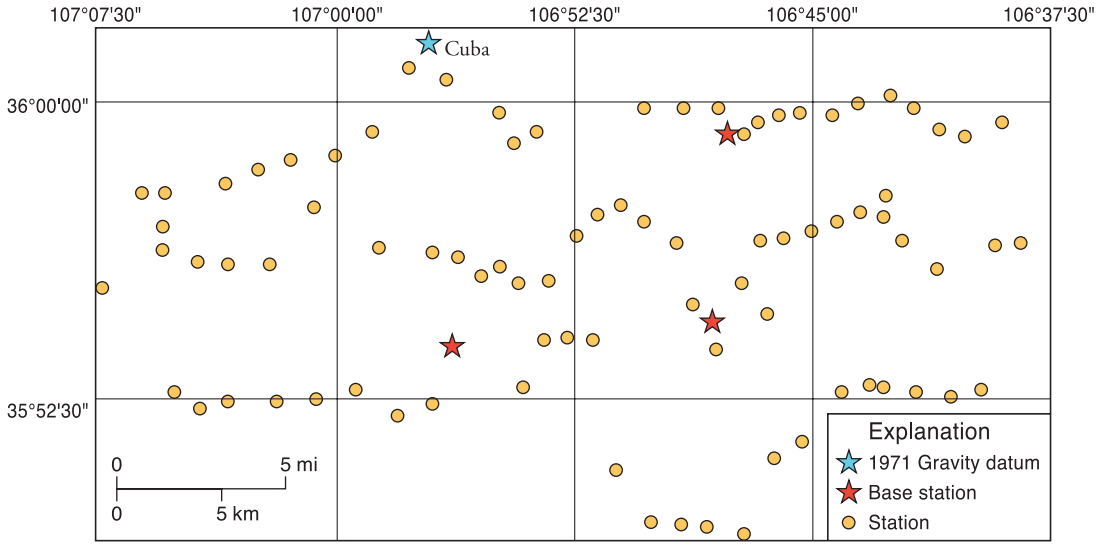


FIGURE 7—Location map for gravity measurements and base stations.

Warburton (1986) refer to structures such as these as passive backthrusts. This type of structure is observed in the Laramide Rattlesnake Mountain and Forellen Peak structures (Erslev and Rogers 1993)

**Strike sections**

Sections C–C′ and D–D′ (Sheet 4) are drawn parallel to the Nacimiento fault and demonstrate how structures in the subsurface link together along strike. Strike section C–C′ (Sheet 4) crosses from the footwall to the hanging wall of the Nacimiento fault near Location 5 Sheet 1. The line of section for strike section D–D′ lies entirely to the east of the surface trace of the Nacimiento fault.

**Strike section C–C′**—In section C–C′ the wedge-boundary fault is interpreted to deepen to the south. This is a consequence of the southward plunge of the hinge line of the footwall syncline, which we interpret to be located at the leading edge of the block of Joaquin granite (compare the depths of this hinge on sections A–A′ and B–B′). The southward shallowing of the fault at the top of the block of Joaquin granite, the Los Piños fault, can be seen in the field (Sheet 1). The convergence of these two fault surfaces results in significant thinning of the Joaquin granite block to the north. Although not visible on the strike sections, the Joaquin granite block must also thin to the south.

Above the Los Piños fault, the Permian Abo and Yeso Formations in section C–C′ appear to thicken to the south. This is an apparent thickness change caused by progressive steepening of the bedding southward. The appearance of the Nacimiento fault on section C–C′ occurs where the line of section crosses the surface trace of the fault. The strata in the hanging wall of the Nacimiento fault dip to the north and are truncated by the east-dipping Nacimiento fault. The Nacimiento fault is climbing higher into the section to the north, and, although not shown on the cross section, it soles into the Salitral Shale Member (Location 10 Sheet 1). This geometry indicates that there is a lateral ramp preserved in the hanging wall of the Nacimiento fault.

**Strike section D–D′**—The faults in section C–C′ are also present in section D–D′; however, there are slight differences in their geometry and position within the sections. As in section C–C′, the wedge-boundary fault deepens to the south in section D–D′. The Joaquin granite block is thinner in section D–D′ than in C–C′ because this line of section is farther east and is nearer the branch line between the wedge-boundary fault and the Nacimiento fault (see Sheets 2, 3). In section C–C′ the Los Piños fault is below the Nacimiento fault, and in section D–D′ the Los Piños fault is above the Nacimiento fault. This is because the Los Piños fault is cut by the Nacimiento fault and is in the hanging wall of the Nacimiento fault in D–D′ and in the footwall in C–C′ (see Sheet 2).

## Gravity modeling

**Bouguer gravity map**

A Bouguer gravity map was constructed using data gathered along three traverses across the western margin of the Sierra Nacimiento uplift (Wallace 1996; Fig. 7). Traverses began in the San Juan Basin, approximately 11 km west of the uplift and extended across the Sierra Nacimiento uplift into the Jemez Mountains, 13 km east of the trace of the Nacimiento fault. Data for 91 stations were collected using a Model #124 Worden gravimeter. Our gravity survey covered parts of the Headcut Reservoir, Mesa Portales, La Ventana, San Pablo, Cuba, San Miguel Mountain, Rancho del Chaparral, Jarosa, and Seven Springs 7.5-min quadrangles. In all three traverses gravity was measured at stations spaced about 0.8–2.4 km apart.

Our gravity measurements are tied to the 1971 gravity base station located at the flagpole on the southeast corner of the old Cuba, New Mexico, post office. This building is now a grocery store and is located on the west side of US–550 just south of the intersection with NM–126. The established gravitational value at this station is 979,165.36 mgal. We used this base station to calibrate our measurements and to correct for instrument drift. Additional base stations were established within the study area to permit frequent recalibration of the gravimeter during data acquisition (Fig. 7).

Station data from the survey were reduced to the Bouguer gravity anomaly using the BOUGUER software (Goodson and Plouff 1988), which performed the terrain, latitude, longitude, free-air, and Bouguer corrections. The resulting Bouguer gravity data are tabulated in Appendix A, and a contour map was generated using MacGRIDZO (Fig. 8). The contour patterns of our Bouguer gravity map are similar to those shown by Keller and Cordell (1984) for this area. However, the higher density of control points used to generate our map allows us to investigate finer-scale anomalies

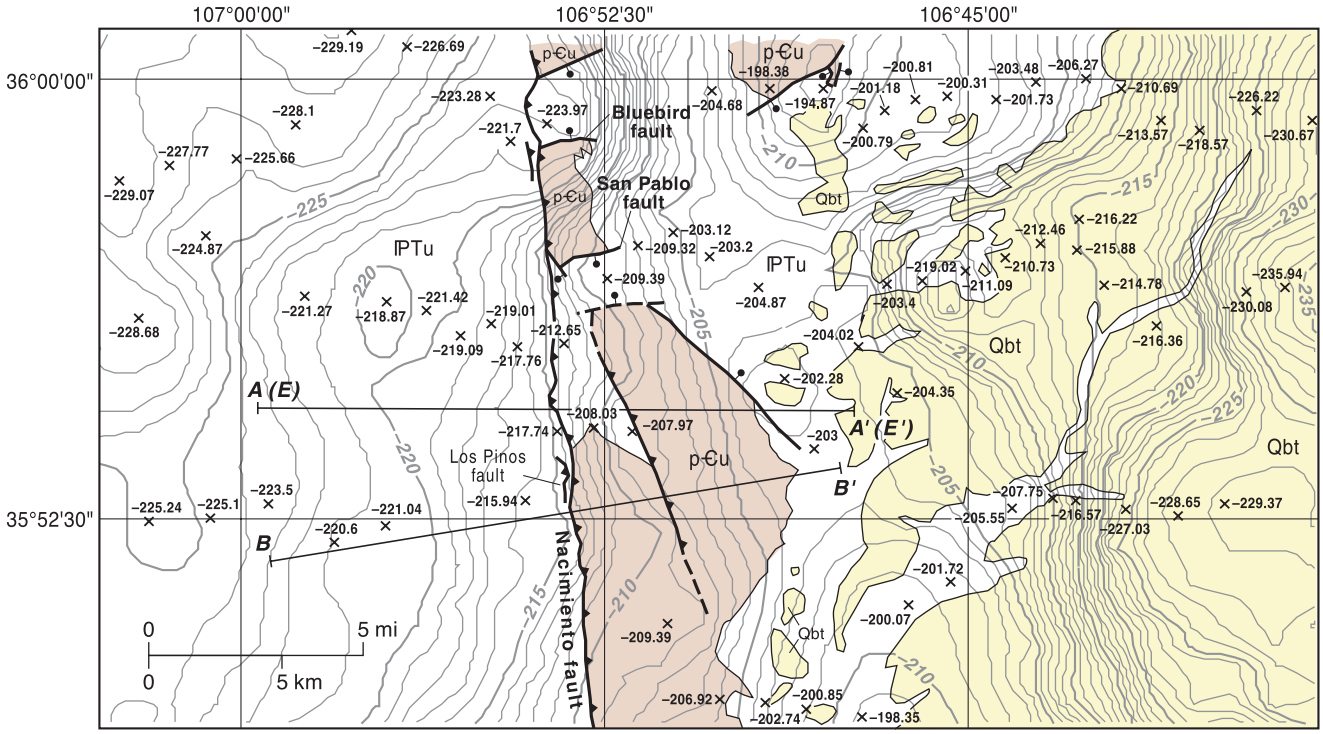


FIGURE 8—Bouguer gravity map overlain on generalized bedrock geologic map of the Sierra Nacimiento uplift. Line **A(E)–A′(E′)** is observed Bouguer gravity profile in Figures 9 and 10.

and their underlying structures. The overall trend of the Bouguer anomaly values shows a rise from about – 230 mgals at the western edge of the map to about – 205 mgals on the crest of the Sierra Nacimiento, which is due to the strong density contrast between the low density rocks of the San Juan Basin and the elevated crystalline rocks of the uplift. Farther east there is a precipitous drop in the anomaly values to about – 235 mgals, which corresponds to the western edge of the Valles caldera and is caused by the great thickness of low density tuff (Nielson and Hulen 1984) and possibly elevated temperatures related to the volcanism (Ankeny et al. 1986).

Within these large-scale trends there are some smaller-scale gravity features that can be correlated to the mapped geology. In the northern part of the map area, the east-west graben defined by the Bluebird and El Cajete faults corresponds to a reentrant in the contour pattern, which is caused by the relative density contrast between the sedimentary rocks within the graben and the crystalline basement of the adjacent horst blocks. The steep rise in the gravity at the eastern end of the graben does not correspond to any mapped feature and may be reflecting a buried, high-angle fault within the crystalline basement. A second transverse graben bounded by the San Pablo fault to the north and an unnamed fault to the south does not correspond to a reentrant in the gravity contours, suggesting that the basement is structurally higher than within the northern graben.

At a latitude of 35°52′30″ slightly higher gravity values west of the Nacimiento fault correspond to the elevated block of crystalline basement beneath the footwall culmination. South of this area the gravity contours appear to be elevated, however, this trend is an artifact of the contouring algorithm used by MacGRIDZO.

### Gravity models of the central Sierra Nacimiento

Bouguer anomaly values from profile E–E′ were used in the GRAV2D® gravity modeling software. This software calculates a gravity profile from a geologic model, which can be compared to the measured gravity data. Gravity profile line E–E′ is coincident with structural cross section A–A′, which was chosen because gravity contours along this line are better constrained. Model densities for the Cretaceous and Jurassic sedimentary units were determined from a compensated density log from the Nuclear Corporation of New Mexico La Ventana No. 1 well located in the SW¼ SW¼ sec. 14 T19N R1W. Densities for the sedimentary units not penetrated by this well were obtained from Anderson (1955), Mattick (1967), Ramberg et al. (1978), and Toth et al. (1993). Crystalline basement rocks were assumed to have a density of 2.67 g/cm$^3$.

Woodward's (1987) cross section through this area (section C–C′; sheet 1 in Woodward 1987) shows a high-angle contact between the sedimentary rocks of the San Juan Basin and the crystalline rocks of the Sierra Nacimiento uplift. A gravity model based on this cross section is shown in Figure 9. A structurally deep, high-angle contact between basement and sedimentary rocks results in a gravity gradient across the fault that is too steep and is a poor match to the observed gravity. A gravity model based on cross section A–A′ from this study, however, results in a calculated gravity profile that correlates well with the observed gravity (Fig. 10). This gravity model along with our dip information supports our interpretation that a basement wedge is faulted beneath the sedimentary rocks in the footwall of the Nacimiento fault.

### Structural evolution of the Sierra Nacimiento

Dextral slip followed by vertical uplift has endured as the kinematic model of the Sierra Nacimiento for several decades (Kelley 1955; Baltz 1967; Woodward et al 1972; Chapin and Cather 1983; Woodward 1987). The earliest workers in the Nacimiento interpreted the Nacimiento fault to be an overthrust (Renick 1931; Wood and Northrop 1946). Later workers reinterpreted the Nacimiento fault to be a

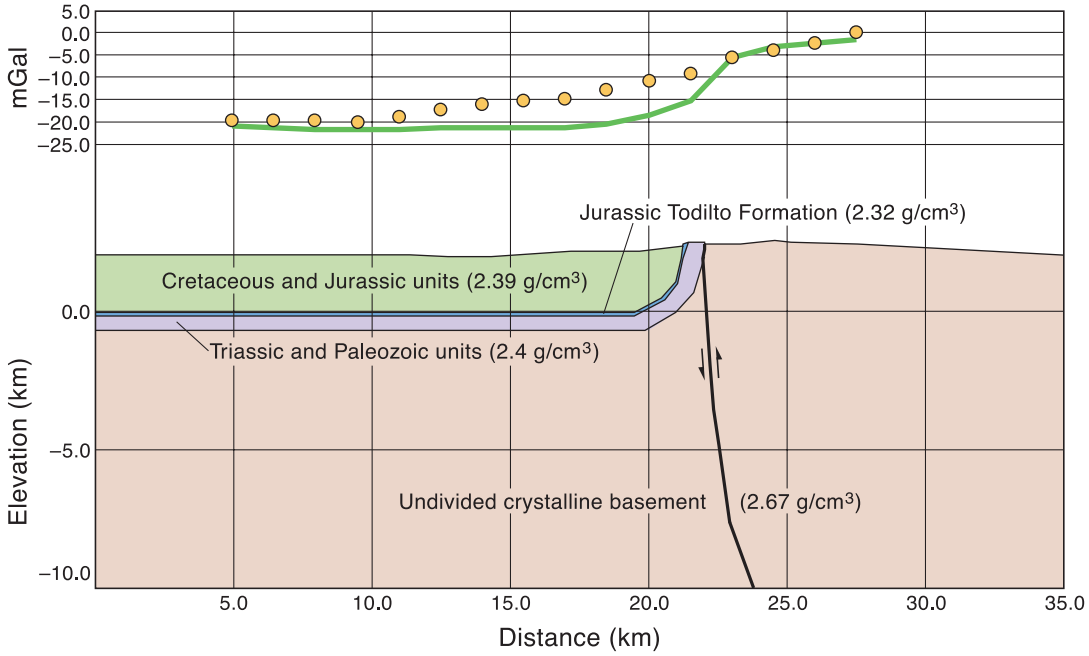


FIGURE 9—Gravity model for upthrust interpretation of the Sierra Nacimiento uplift. Circles are the measured complete Bouguer anomaly values; the solid line is the complete Bouguer anomaly profile calculated from geologic model below. This plot shows the poor fit between measured gravity and gravity profile corresponding to a high-angle fault.

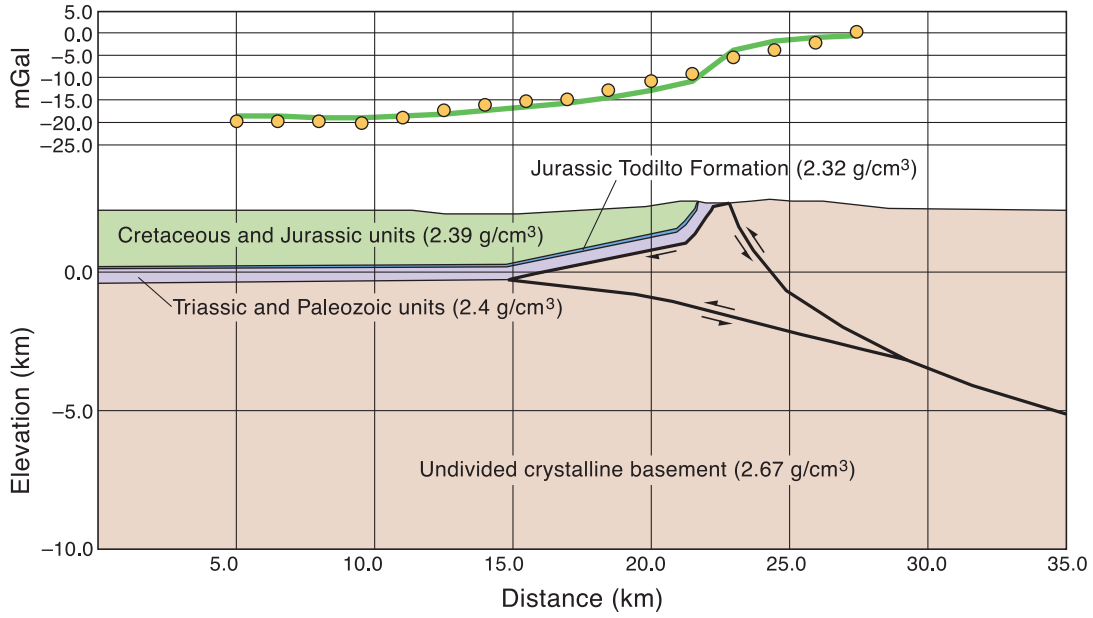


FIGURE 10—Gravity model for cross section **A–A′** (Sheet 2). Circles are the measured complete Bouguer anomaly values; the solid line is the complete Bouguer anomaly profile calculated from geologic model below. This plot shows the good fit between this interpretation of the deep structure and measured gravity.

result of primarily vertical uplift based on the steep dip of the fault generally observed in outcrop and the linear trace of the fault along the mountain front (Baltz 1967; Woodward et al. 1972; Woodward 1987). The kinematic model developed in this study also contains an early strike-slip event; however, we interpret the uplift to be a result of primarily horizontal shortening.

**Dextral strike-slip**

The amount of dextral slip along the Nacimiento fault system has been difficult to quantify. Chapin and Cather (1983) used the magnitude of shortening in the Wyoming province of the Rockies to estimate 77–110 km of dextral displacement between the Colorado Plateau and the craton to the east. Karlstrom and Daniel (1993) suggested that 100–170 km of right-lateral displacement between the North American craton and the Colorado Plateau (30 km on the Nacimiento fault) could be demonstrated using offset Precambrian intrusions and isobaric surfaces. Woodward et al. (1997) interpreted that only 5–20 km of right slip is

allowed by east-trending depositional pinchouts and isopach lines of Jurassic and Cretaceous strata, although this interpretation is based on pinchouts that are not tightly constrained by control points. Cather (1999) cites the offset stratigraphic pinchout of the Upper Cretaceous Gallup Sandstone as evidence for 20–33 km of dextral slip on the Sand Hill–Nacimiento fault system. Baltz (1967) cited the folding of the San Juan Basin strata as evidence for about 5 km of dextral slip on the Nacimiento fault. Baltz (1967) also noted that the eastward step of the dextral strike-slip Nacimiento fault at Gallina (Fig. 2) should produce extensional faulting. If there has been large dextral displacement on the present trace of the Nacimiento fault, large amounts of extension would be observed in this releasing bend in the Nacimiento fault system. The lack of extensional structures with significant displacements in the vicinity of Gallina was cited by Baltz (1967) as supporting evidence for only 5 km of dextral offset on the Nacimiento fault. Alternatively, if most of the motion on the present trace of the Nacimiento fault is west-directed thrusting then the east trending segment of the Nacimiento fault at Gallina would correspond to an edge of the thrust sheet eliminating the need for extension as proposed by Baltz (1967).

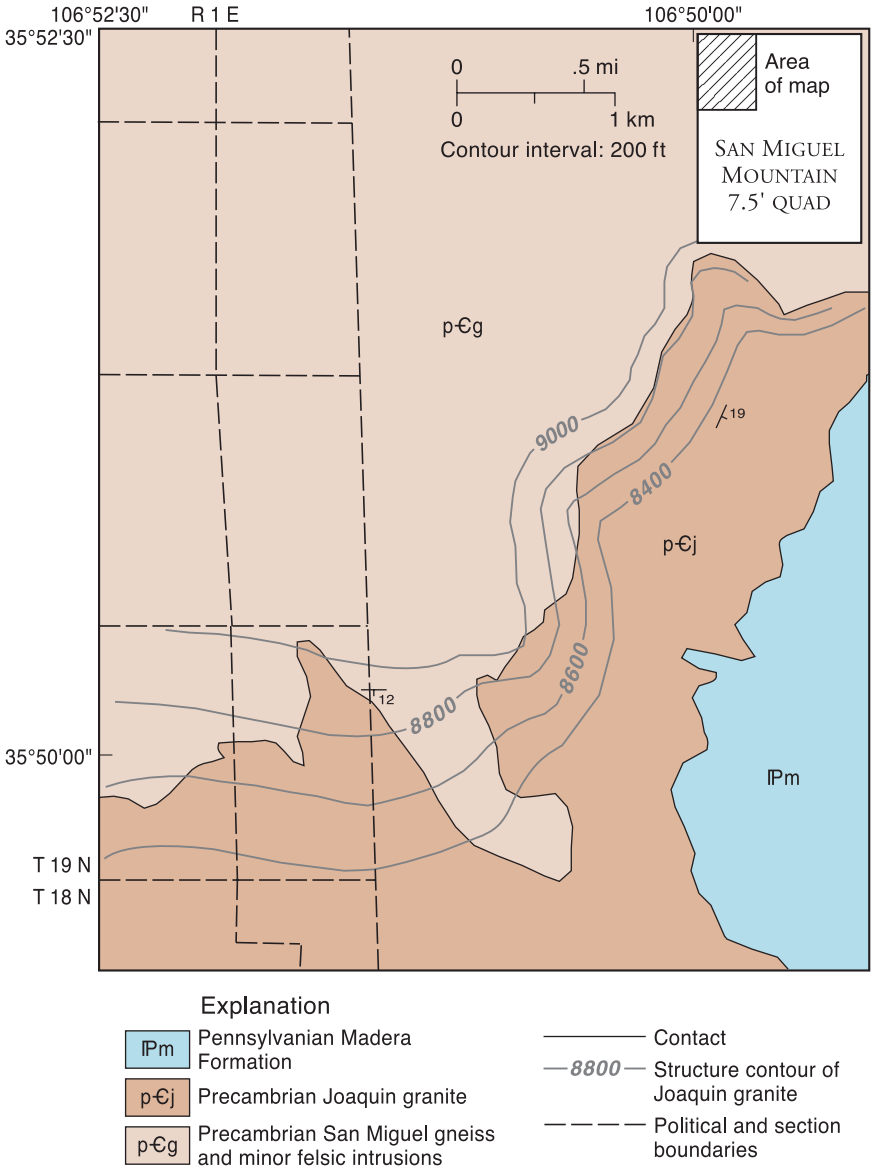


FIGURE 11—Structure contour map of the Precambrian San Miguel gneiss–Joaquin granite contact. Geologic data are from Woodward et al. (1974).

In this study we use an offset geologic unit that is in contact with the Nacimiento fault in both the hanging-wall and footwall blocks. The block of Joaquin granite discovered in the footwall of the Nacimiento fault (Sheet 1) appears to have been displaced from a large body of Joaquin granite located in the hanging wall to the south (see Fig. 2). The northernmost exposure of the granite in the hanging wall is 6 km to the south of the footwall block of Joaquin granite; the southernmost exposure is 18 km south. The amount of dextral separation between the footwall and hanging wall outcrops of Joaquin granite, therefore, ranges between 6 and 18 km, depending on whether the footwall outcrop came from the northern end or the southern end of the hanging wall exposure. The magnitude of the displacement between the two granite bodies, as opposed to the separation, depends on the orientation of the slip vector on the fault, the orientation of the contact between the granite and surrounding gneiss, and the presence of only one body of Joaquin granite. Structure contours of the northern contact between the granite and gneiss show that it dips gently (8–12°) to the south near its hanging wall cutoff in the La Ventana 7.5-min quadrangle (Fig. 11). For any non-vertical contact strike separation can be achieved through purely dip slip motion, purely strike slip motion, or some combination of the two. Figure 12 shows end-member cases for achieving both 6 and 18 km of strike separation by purely dip slip motion and purely strike slip motion for a contact with a 12° dip to the south. For the dip-slip fault, 6 km of separation is produced by 1 km of dip-slip motion; 18 km of separation requires 3 km of dip-slip. From cross section B–B′, we estimate 0.5 km of dip-slip motion on the Nacimiento fault based on the footwall and projected hanging wall cutoffs of the Pennsylvanian Madera Formation (Sheet 3). This translates to 3 km of dextral strike separation. Depending on whether the footwall granite came from the northern or southern end of the hanging wall granite, the amount of pure dextral strike-slip motion on the Nacimiento fault system is between 3 and 15 km (Figs. 13, 14).

The timing of the dextral slip along the Nacimiento fault is also controversial. Estimates of dextral slip by Karlstrom and Daniel (1993) and Daniel et al. (1995) are based on offset Proterozoic features and cannot be directly tied to Laramide tectonics. Cather's (1999) and Woodward et al.'s (1997) estimates of dextral slip are based on offset Mesozoic strata and are presumably Laramide. Woodward (1996) proposed that the disparity between his lower estimates of Laramide dextral slip (5 km) along the Nacimiento fault and the estimates of 20 km or more by Karlstrom and Daniel (1993) using Proterozoic features can be resolved by partitioning some of the dextral slip into an earlier event associated with the late

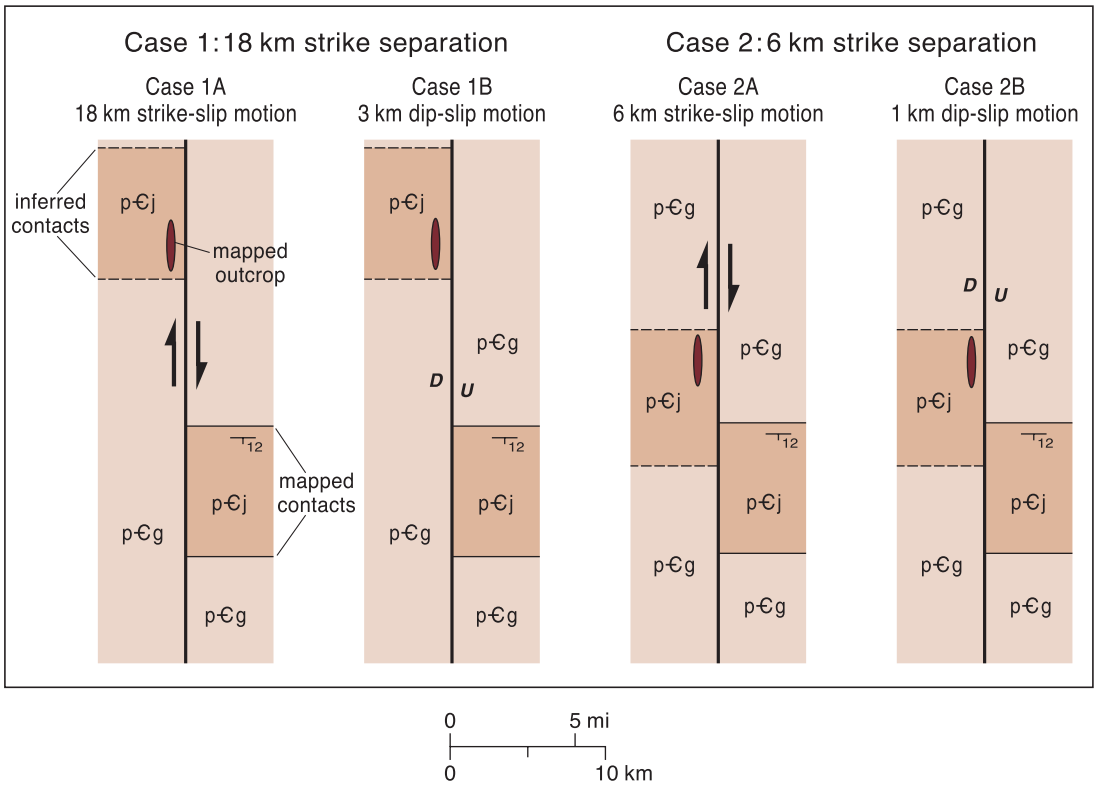


FIGURE 12—Diagrams showing strike separation of the Joaquin granite by strike-slip and dip-slip motion. Mapped contacts of Joaquin granite are shown with solid lines; inferred contacts are shown with dashed lines. Joaquin granite outcrop from Sheet 1 is shown as ellipse. The maximum strike separation of 18 km (Case 1) and minimum strike separation of 6 km (Case 2) correspond to different locations of the Joaquin granite outcrop within the larger body west of the fault. Cases 1A and 2A show pure strike-slip displacement across the fault. Cases 1B and 2B show pure dip-slip displacement across the fault.

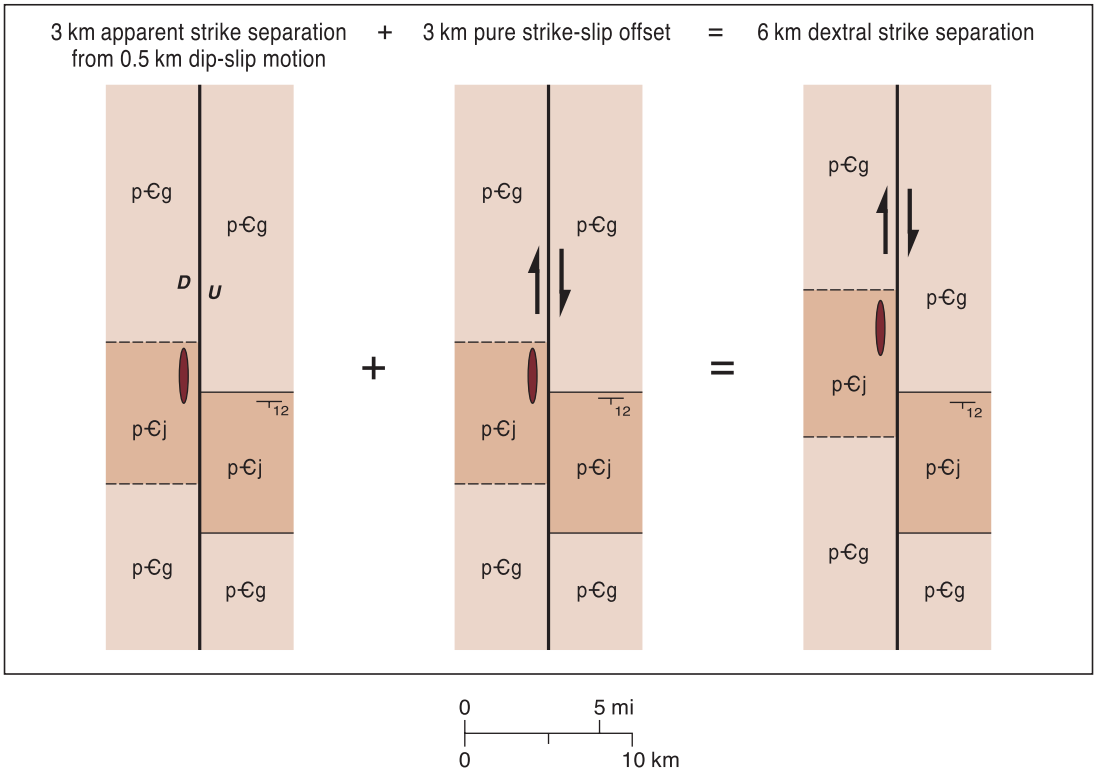


FIGURE 13—Diagram showing minimum dextral displacement on the Nacimiento fault. The 0.5 km (of dip-slip motion on the Nacimiento fault is obtained from cross section B–B′ (Sheet 3). This dip-slip motion produces 3 km of strike separation. An additional 3 km of pure strike-slip displacement is required to produce the minimum strike separation of 6 km.

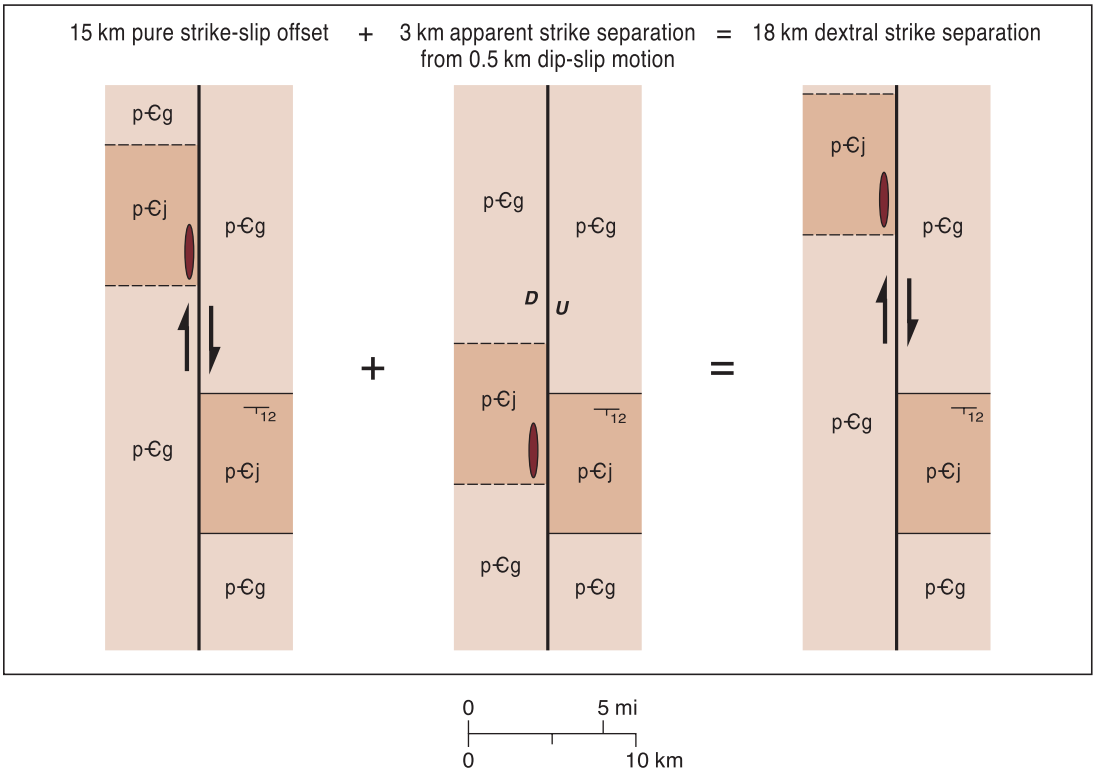


FIGURE 14—Diagram showing maximum dextral displacement on the Nacimiento fault. The 18 km of strike separation is produced by 0.5 km of dip-slip motion combined with 15 km of strike-slip motion.

Paleozoic Peñasco uplift, which coincided with the present day Sierra Nacimiento uplift. Because our offset marker is a Precambrian granite, we can only constrain the dextral slip to be post-Joaquin granite intrusion; however, we believe that the dextral motion on the Nacimiento fault system occurred before the main east-west shortening event during early stages of the Laramide or perhaps even earlier. If dextral slip occurred on the Nacimiento fault system synchronous with Laramide shortening, the four slickenlines we observed should show a significant component of north-south motion. In addition it is unlikely that the nearly flat, west-directed thrust fault in the northern part of the map area (Sheet 1) would have been preserved if there had been major north-south strike-slip motion on this same fault surface. Hultgren (1986) observed kinematic indicators showing primarily dip-slip motion on the northern part of the Sierra Nacimiento, suggesting that the absence of strike-slip motion is not restricted to our map area.

### Dip slip

Fold axes of the en echelon north-northwest-trending folds in San Juan Basin sediments are cut by the uplift and are folded in the lower limb of the monocline, suggesting that the dip-slip motion occurred after strike-slip motion (Baltz 1967; Woodward 1987). The uplift event in this field area is also constrained by apatite fission-track cooling ages obtained by Kelley et al. (1992). Although there is a wide range in cooling ages, most of the rocks in the hanging wall of the Nacimiento fault cooled to below ~ 100 °C by the late Eocene.

Lineations from both the low-angle (Giral 1995) and high-angle (Fig. 5) parts of the Nacimiento fault generally trend east-west indicating dip-slip motion. These kinematic indicators suggest that for this part of the uplift the latest motion along the Nacimiento fault system was primarily dip slip.

As mentioned previously the basement-cover interface acts as a décollement in the forelimb of the structure. In section A–A′ (Sheet 2) this surface is shown as the top-to-the-east Los Piños fault. The Los Piños fault formed early in the development of the uplift as the basement material began to imbricate beneath it. The Los Piños fault was later folded and faulted by continued motion of deeper basement faults. Late in the contractional development of the uplift, the largest hanging wall block was exhumed on the out-of-sequence high-angle San Miguel reverse fault (Sheets 2, 3). The out-of-sequence faulting of the hanging wall probably exploits preexisting structures within the crystalline basement (e.g., ancestral strike-slip faults). The Trail Creek normal fault could have formed during contraction to accommodate bending of the hanging wall over the footwall ramp. Alternatively, the Trail Creek fault could have formed following cessation of contraction by gravitational collapse of overthickened basement or during subsequent rifting.

## Summary

The cross sections presented in this study provide a kinematically and geometrically acceptable model for the deep structure of the Sierra Nacimiento uplift. Contrary to earlier structural interpretations our model incorporates both low-angle and high-angle faults into an episode of subhorizontal tectonic shortening. The validity of these cross sections is supported by gravity modeling, which shows that the gradual rise in gravity across the mountain front can be explained by underthrusting of a basement wedge beneath the sedimentary cover of the adjacent San Juan Basin. The gravity signature is incompatible with the downward-steepening basement faults shown in earlier cross sections by Woodward (1987) accommodating vertical uplift. An alternative mechanism to generate the fault geometries observed along the Nacimiento is that of partitioned dextral transpression. However, we believe that the west-vergent asym-

metry and the apparent diachroneity of the strike-slip and dip-slip faults argue against this mechanism.

Assuming that they were not originally separate bodies a granitic pluton cut by the Nacimiento fault provides a marker, which indicates 3–15 km of pre- or early-Laramide dextral slip along the Nacimiento fault. Both this north-south, dextral-slip vector combined with the Laramide east-west, dip-slip vector of about 7 km provides constraints on the motion of the Colorado Plateau with respect to the Sierra Nacimiento. The total motion between the Colorado Plateau and the North American craton has been accommodated on faults to the east of the Nacimiento fault (Karlstrom and Daniel 1993). Further studies that constrain timing of the motion on the Nacimiento fault and faults to the east are necessary to truly constrain the motion of the Colorado Plateau with respect to the North American craton.

## Acknowledgments

Financial support for this project was provided by Department of Geological Sciences, University of North Carolina at Chapel Hill, Martin Research Fellowships, and Geological Society of America grants to both Caleb Pollock and Ruben Giral; a grant from the Colorado Scientific Society to Caleb Pollock; and a University of North Carolina at Chapel Hill Honors Program Science Opportunities Fellowship to Laura Wallace.

This manuscript was greatly improved by the thoughtful comments of E. A. Erslev, L. A. Woodward, and S. M. Cather. Thanks also to William Watley and Stewart Gauchupin of the Jemez Department of Natural Resources for assisting us with access to the Holy Ghost Springs area of the Jemez land grant.

## References

Anderson, R. C., 1955, A gravity survey of the Rio Grande trough near Socorro, New Mexico: American Geophysical Union, Transactions, v. 36, no. 1, pp. 144–148.

Ankeny, L. A., Braile, L. W., and Olsen, K. H., 1986, Upper crustal structure beneath the Jemez Mountains volcanic field, New Mexico, determined by three-dimensional simultaneous inversion of seismic refraction and earthquake data: Journal of Geophysical Research, v. 91, no. B6, pp. 6188–6198.

Baltz, E. H., 1967, Stratigraphy and regional tectonic implications of part of Upper Cretaceous and Tertiary rocks, east-central San Juan Basin, New Mexico: U.S. Geological Survey, Professional Paper 552, 101 pp.

Banks, C. J., and Warburton, J., 1986, "Passive-roof" duplex geometry in the frontal structures of the Kirthar and Sulaiman mountain belts, Pakistan: Journal of Structural Geology, v. 8, no. 3/4, pp. 229–237.

Brown, W. G., 1988, Deformational style of Laramide uplifts in the Wyoming foreland; *in* Schmidt, C. J., and Perry, W. J., Jr. (eds.), Interaction of the Rocky Mountain foreland and the Cordilleran thrust belt: Geological Society of America, Memoir 171, pp. 1–52.

Cather, S. M., 1996, Laramide oblique-slip faulting in New Mexico—an overview (abs.): Geological Society of America, Abstracts with Programs, v. 28, no. 7, p. A-374.

Cather, S. M., 1999, Implications of Jurassic, Cretaceous, and Proterozoic piercing lines for Laramide oblique-slip faulting in New Mexico and rotation of the Colorado Plateau: Geological Society of America, Bulletin, v. 111, no. 6, pp. 849–868.

Chapin, C. E., and Cather, S. M., 1983, Eocene tectonics and sedimentation in the Colorado Plateau–Rocky Mountain area; *in* Lowell, J. D., and Gries, R. R. (eds.), Rocky Mountain foreland basins and uplifts: Rocky Mountain Association of Geologists, pp. 33–56.

Daniel, C. G., Karlstrom, K. E., Williams, M. L., and Pedrick, J. N., 1995, The reconstruction of a middle Proterozoic orogenic belt in north-central New Mexico, U.S.A.; *in* Bauer, P. W., Kues, B. S., Dunbar, N. W., Karlstrom, K. E., and Harrison, B. (eds.), Gelogy of the Santa Fe region: New Mexico Geological Society, Guidebook 46, pp. 193–200.

Erslev, E. A., 1986, Basement balancing of Rocky Mountain foreland uplifts: Geology, v. 14, pp. 259–262.

Erslev, E. A., 1993, Thrusts, back-thrusts, and detachment of Rocky Mountain foreland arches; *in* Schmidt, C. J., Chase, R. B., and Erslev, E. A. (eds.), Laramide basement deformation in the Rocky Mountain foreland of the western United States: Geological Society of America, Special Paper 280, pp. 339–358.

Erslev, E. A., and Rogers, J. L., 1993, Basement-cover geometry of Laramide fault-propagation folds; *in* Schmidt, C. J., Chase, R. B., and Erslev, E. A. (eds.), Laramide basement deformation in the Rocky Mountain foreland of the western United States: Geological Society of America, Special Paper 280, pp. 125–146.

Evans, J. P., 1986, Comment on "Basement balancing of Rocky Mountain foreland uplifts": Geology, v. 14, p. 806.

Giral, R. A., 1995, Early structural evolution of a Laramide uplift, Sierra Nacimiento, New Mexico: Unpublished M.S. thesis, University of North Carolina at Chapel Hill, 53 pp.

Godson, R., and Plouff, D., 1988, BOUGUER version 1.0 a microcomputer gravity-terrain-correction program: U.S. Geological Survey, Open-file Report, 88-644A, 132 pp.

Gordy, P. L., Frey, F. R., and Norris, D. K., 1977, Geological guide for the Canadian Society of Petroleum Geologists and 1977 Waterton-Glacier Park field conference: Canadian Society of Petroleum Geologists, Calgary, 93 pp.

Hamilton, W., 1978, Mesozoic tectonics of the western United States; *in* Howell, D. G., and McDougal, K. (eds.), Mesozoic paleogeography of the United States: Society of Economic Paleontologists and Mineralogists, Pacific Section, Pacific Coast Paleogeography Symposium, no. 2, pp. 33–70.

Hultgren, M. C., 1986, Tectonics and stratigraphy of the southern Gallina–Archuleta arch, French Mesa and Llaves quadrangles, Rio Arriba County, New Mexico: Unpublished M.S. thesis, University of New Mexico, 123 pp.

Karlstrom, K. E., and Daniel, C. G., 1993, Restoration of Laramide right-lateral strike slip in northern New Mexico by using Proterozoic piercing points—tectonic implications from the Proterozoic to the Cenozoic: Geology, v. 21, no. 9, pp. 1139–1142.

Keller, G. R., and Cordell, L., 1982, Complete Bouguer gravity anomaly map of New Mexico: National Oceanic and Atmospheric Administration, National Geophysical Data Center, scale 1:500,000.

Kelley, S. A., Chapin, C. E., and Corrigan, J., 1992, Late Mesozoic to Cenozoic cooling histories of the flanks of the northern and central Rio Grande rift, Colorado and New Mexico: New Mexico Bureau of Mines and Mineral Resources, Bulletin 145, 40 pp.

Kelley, V. C., 1955, Regional tectonics of the Colorado Plateau and the relationship to the origin and distribution of uranium: University of New Mexico, Publications in Geology, no. 5, 122 pp.

Laughlin, A. W., Eddy, A. C., Laney, R., and Aldrich, M. J., Jr., 1983, Geology of the Fenton Hill, New Mexico, Hot Dry Rock site: Journal of Volcanology and Geothermal Research, v. 15, no. 1-3, pp. 21–41.

Mattick, R. E., 1967, A seismic and gravity profile across the Hueco Bolson, Texas: U.S. Geological Survey, Professional Paper 575-D, pp. 85–91.

Nielson, D. L., and Hulen, J. B., 1984, Internal geology and evolution of the Redondo dome, Valles caldera, New Mexico: Journal of Geophysical Research, v. 89, no. 10, pp. 8695–8711.

Prucha, J. J., Graham, J. A., and Nickelsen, R. P., 1965, Basement-controlled deformation in Wyoming province of Rocky Mountain foreland: American Association of Petroleum Geologists, Bulletin, v. 49, no. 7, pp. 966–992.

Ramberg, I. B., Cook, F. A., and Smithson, S. B., 1978, Structure of the Rio Grande rift in southern New Mexico and western Texas based on gravity interpretation: Geological Society of America, Bulletin, v. 89, no. 1, pp. 107–123.

Renick, B. C., 1931, Geology and ground-water resources of western Sandoval County, New Mexico: U.S. Geological Survey, Water Supply Paper 620, 117 pp.

Sanford, A. R., 1959, Analytical and experimental study of simple geologic structures: Geological Society of America, Bulletin, v. 79, no. 1, pp. 19–51.

Slack, P. B., and Campbell, J. A., 1976, Structural geology of the Rio Puerco fault zone and its relationship to central New Mexico tectonics; *in* Woodward, L. A., and Northrop, S. A. (eds.), Tectonics and mineral resources of southwestern North America: New Mexico Geological Society, Special Publication 6, pp. 46–52.

Smithson, S. B., Brewer, J. A., Kaufman, S., Oliver, J. E., and Hurich, C. A., 1979, Structure of the Laramide Wind River uplift, Wyoming, from COCORP deep-reflection data and from gravity data: Journal of Geophysical Research, v. 84, no. B11, pp. 5955–5972.

Stewart, K. G., and Hibbard, J. P., 1992, Low-angle thrust faulting at the eastern edge of the San Juan Basin associated with the Nacimiento uplift; *in* Lucas, S. G., Kues, B. S., Williamson, T. E., and Hunt, A. P. (eds.), San Juan Basin IV: New Mexico Geological Society, Guidebook 43, pp. 7–9.

Suppe, J., 1985, Principals of structural geology: Prentice-Hall Inc., 537 pp.

Taylor, D. J., and Huffman, A. C., Jr., 1998, Map showing inferred and mapped basement faults, San Juan Basin and vicinity, New Mexico and Colorado: U.S. Geological Survey, Geologic Investigations Series I-2641, scale 1:500,000.

Toth, M. I., Wilson, A. B., Cookro, T. M., Bankey, V., Lee, G. K., and Case, J. E., 1993, Mineral resource potential and geology of the White River National Forest and the Dillon Ranger District of the Arapahoe National Forest, Colorado: U.S. Geological Survey, Bulletin 2035, 117 pp.

Wallace, L. M., 1996, Gravity survey of the Nacimiento Mountains, north-central New Mexico: Unpublished honors thesis, University of North Carolina at Chapel Hill, 46 pp.

Wood G. H., Northrop, S. A., and Cowen, M. J., 1946, Geology of the Nacimiento Mountains, San Pedro Mountain, and adjacent plateaus in parts of Sandoval and Rio Arriba Counties, New Mexico: U.S. Geological Survey, Oil and Gas Investigations Map OM-57, scale 1:95,000.

Woodward, L. A., 1987, Geology and mineral resources of Sierra Nacimiento and vicinity, New Mexico: New Mexico Bureau of Mines and Mineral Resources, Memoir 42, 84 pp.

Woodward, L. A., and Schumacher, O., 1973, Geologic map and sections of La Ventana quadrangle, New Mexico: New Mexico Bureau of Mines and Mineral Resources, Geologic Map GM-28, scale 1:24,000.

Woodward, L. A., Anderson, O. J., and Lucas. S. G., 1997, Mesozoic stratigraphic constraints on Laramide right slip on the east side of the Colorado Plateau: Geology, v. 25, no. 9, pp. 843–846.

Woodward, L. A., DuChene, H. R., and Reed, R. K., 1974, Geologic map and sections of San Miguel Mountain quadrangle, New Mexico: New Mexico Bureau of Mines and Mineral Resources, Geologic Map GM-34, scale 1:24,000.

Woodward, L. A., Kaufman, W. H., and Anderson, J. B., 1972, Nacimiento fault and related structures, northern New Mexico: Geological Society of America, Bulletin, v. 83, no. 8, pp. 2383–2396.

Woodward, L. A., Kaufman, W. H., and Reed, R. K., 1973b, Geologic map and sections of Rancho del Chaparral quadrangle, New Mexico: New Mexico Bureau of Mines and Mineral Resources, Geologic Map GM-27, scale 1:24,000.

Woodward, L. A., Anderson, J. B., Kaufman, W. H., and Reed, R. K., 1973a, Geologic map and sections of San Pablo quadrangle, New Mexico: New Mexico Bureau of Mines and Mineral Resources, Geologic Map GM-26, scale 1:24,000.

Yin, A., and Ingersoll, R. V., 1997, A model for evolution of Laramide axial basins in the southern Rocky Mountains, USA: International Geology Review, v. 39, no. 10, pp. 1113–1123.